This is a repository copy of *A new predictive model for normal and compound impact wear*.

White Rose Research Online URL for this paper:
https://eprints.whiterose.ac.uk/174474/

Version: Accepted Version

Article:
Zalzalah, M. orcid.org/0000-0001-5712-5531, Lewis, R. orcid.org/0000-0002-4300-0540 and Slatter, T. orcid.org/0000-0002-0485-4615 (2021) A new predictive model for normal and compound impact wear. Wear, 480-481. 203954. ISSN 0043-1648

https://doi.org/10.1016/j.wear.2021.203954

© 2021 Elsevier. This is an author produced version of a paper subsequently published in Wear. Uploaded in accordance with the publisher's self-archiving policy. Article available under the terms of the CC-BY-NC-ND licence (https://creativecommons.org/licenses/by-nc-nd/4.0/).

Reuse
This article is distributed under the terms of the Creative Commons Attribution-NonCommercial-NoDerivs (CC BY-NC-ND) licence. This licence only allows you to download this work and share it with others as long as you credit the authors, but you can't change the article in any way or use it commercially. More information and the full terms of the licence here: https://creativecommons.org/licenses/

Takedown
If you consider content in White Rose Research Online to be in breach of UK law, please notify us by emailing eprints@whiterose.ac.uk including the URL of the record and the reason for the withdrawal request.

eprints@whiterose.ac.uk
https://eprints.whiterose.ac.uk/

A New Predictive Model for Normal and Compound Impact Wear

Mohanad Zalzalah, Roger Lewis, Tom Slatter*

Department of Mechanical Engineering, The University of Sheffield, Mappin Street,

Sheffield, U.K. S1 3JD

* Corresponding author – tom.slatter@sheffield.ac.uk

Abstract

This work presents a new model that predicts the wear that results from impacts occurring between two solid bodies under both normal and compound impact, a capability lacking from existing approaches. This frequently occurs in many engineering and industrial situations and depending on the relative sizes of the bodies, bulk material properties, and the number and frequency of impacts, damage can result. Although this eventually causes severe wear problems that limit service life, it is one of the least investigated types of primary wear mechanism. Due to this, robust data, and validated models derived from that data, are rare.

The new model considers the contact with respect to shear force. It can predict wear volume loss and be used to improve understanding of the role of different impact angles during impact, and thus inform the design of machines, however it is currently valid for ductile materials only since hardness is a parameter. Empirical inputs to the model were developed using data produced specifically for this work. Predictions made by the model were then validated, with good correlation, for three common metal alloys by means of comparison with experimental data available in the literature.

Keywords: impact wear; impact wear modelling; impact angle, sliding wear, compound impact

Nomenclature

A	Contact area after N cycles (mm^2)
A_i	Initial elastic contact area(mm^2)
e	Impact energy (J)
F	Applied Force (N)
$\overline{F}$	Average Force (N)
F_n	Normal component of impact force (N)
F_t	Tangential component of impact force (N)
G	Shear modulus or modulus of rigidity (MPa)
H_s	Hardness of the softer material (N/mm^2)/
j	Exponent of contact area ratio
k	Sliding wear coefficient
K	Normal impact wear coefficient
M	The effective mass (kg)
N	Number of cycles (nominal impacts)
$n_{Wellinger}$	Impact wear exponent used in Wellinger's Model
n_{Fricke}	Impact wear exponent used in Fricke's Model
n_{Lewis}	Impact wear exponent used in Lewis' Model
n_{ZLS}	Normal impact wear exponent used in Zalzalah-Lewis-Slatter's Model
m_{ZLS}	Sliding impact wear exponent used in Zalzalah-Lewis-Slatter's Model
R	Ball radius (mm)
R_a	Surface roughness (μm)
V	Impact velocity (mm/s)
V_w	Wear volume
V_t	Total volume loss
W	Wear volume (mm^3)
x	Sliding distance (mm)

Greek Letters

ζ	Energy expended during sliding
μ	Friction coefficient
θ	Impact angle
α, β, γ	Constant impact wear parameters

1 Introduction

Impact between bodies occurs in many situations and analysis of those contacts is typically classified by the bulk nature of the material the bodies (e.g. ‘hard’, ‘soft’, ‘solid’, ‘liquid’), the total number of impacts occurring within the area of interest (e.g. ‘single’, ‘multiple’), and the frequency of each impact (e.g. ‘one-off’, ‘repetitive’). Such impacts may be desired to achieve a specific outcome (e.g. peening, sandblasting) or may be an undesirable root cause of failure, either by near-instant failure from fracture or by progressive damage from wear. Within the context of impacting solid bodies, the latter mechanism is generally categorised by either; damage due to multiple impacts from a large number of smaller solid bodies singularly and collectively impacting on a much larger body (known as erosion or erosive wear), or repetitive impacts from a single solid body on another where the length scales are more similar (known as impact wear).

Impact wear has been formally defined in literature as damage to one solid body due to percussion, which is a repetitive exposure to contact by another, typically solid, body [1]. It is also referred to as: hammering, hammer wear, percussive wear, and other similar terms. Wear and failure prediction are some of the most challenging tasks in the design of materials and their applications, and are often the motivation for research. Without sufficient knowledge of how a material fails, it is difficult to improve its performance or select an alternative material for a particular application.

Impact wear has been a problem since tools were first used [2] and there are many modern industrial machines and processes in which impacting bodies occur. Failures due to wear in these contacts can be costly, for example excessive wear of impacting poppet-type inlet and exhaust valves in internal combustion engines can lead to loss of cylinder pressure, increased emissions, reduced fuel economy and ultimately engine failure [1]. Similar damage also occurs in spring loaded pressure relief valves used in the steam circuits of power generation systems [8] reducing safety and reliability significantly. In wind turbine gearboxes the variable load from the wind causes components to hammer against each other [9] and drastically reduces the service life of these difficult-to-replace components. Failures of tools and machines used for mining coal and other media leads to unnecessary costs associated with regular replacement or refurbishment [10, 11].

Development of the small number of existing impact wear models (as described in Section 2) has been often inspired by approaches used to predict erosive wear, and indeed a number of impact wear models have a similar form to those proposed for erosion. These erosion models are typically presented either as a function of impact velocity [12, 13] or as function of impact energy [2]. The impact wear models are then modified in some way to account for the solid bodies tending to be more similar in size and contacting in a well-defined location, whereas in erosive wear the impinging solid particles tend to be smaller and contact almost randomly with the target surface, often over a much larger area [15]. Comparisons with work considering impact-fretting wear can also be made, but these approaches include the dynamic (vibration) effects [16] which can be neglected for the contacts being considered here.

The impact wear modes illustrated in Figure 1 show that both (b) and (c) involve a small amount of interfacial sliding (small arrow) at the point of contact that the existing models do not directly account for and thus are unable to include in their predictions. The reasons for this are two-fold; firstly, that it is difficult to measure the interfacial sliding distance, and secondly, the requirement to distinguish between genuinely compound impact (impact and sliding occurring simultaneously) and situations where there are separate impact and sliding

events, albeit occurring simultaneously, but it is appropriate to consider the resulting wear holistically for the application about which the model was developed. The vast majority of existing models fall into this latter category, and the remainder account for the wear by means of experimentally derived coefficients unique to that situation. This is also the case with the inclusion of the effect of work hardening.

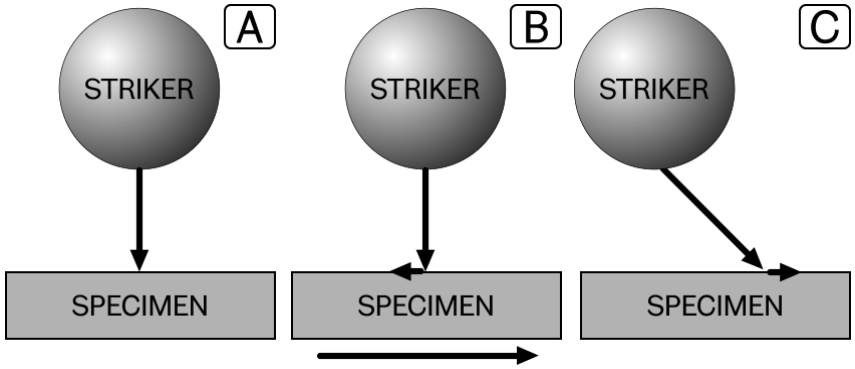

Figure 1 - Different impact wear modes where specimen is under: (a) normal impact (with no sliding), and in compound impact resulting in interfacial sliding due to: (b) striker-specimen relative motion and (c) non-normal impingement angle.

This work proposes a new and experimentally validated model that is able to predict the wear resulting from repetitive impact between two solid bodies at both normal and non-normal angles.

2 Background

2.1 Existing Impact Wear Models

A small number of wear models that claim to be able to predict wear due to impact have been published. They are all semi-empirical and rely on the generation of experimental data to produce accurate predictions. The models are introduced here, and their relative merits then discussed in Section 2.2.

2.1.1 Wellinger & Breckel (1969)

Wellinger & Breckel [12] studied impact wear in normal and dry conditions of various metallic materials (various alloys of steel, aluminium, copper and titanium), using hammering and projectile rigs. Metallic materials were impacted by a spherical hard steel striker head and loads designed to produce plastic deformation from the first impact. The impact velocity used in this work was varied between 0.31-1.72 m/s for a hammering rig and between 3.1-12.7 J for projectile rig, for 5×10^5 and 100 cycles, respectively.

Their subsequent model considers that in the case of ‘soft’ materials (aluminium, copper) which have relatively low hardness and strength, wear is mainly connected with subsurface deformation of the area of impact. whereas with ‘hard’ materials the mechanism of wear is more likely to due to the fracture and subsequent removal of fairly large particles of material. Their analysis of results from mass loss experiments led to the semi-empirical relationship shown in Equation 1.

$$W = KNV^{n_{Wellinger}} \quad (1)$$

where, W represents the wear loss (in mm³), K is a wear coefficient, N is the number of impact cycles, V is the impact velocity (mm/s) and $n_{Wellinger}$ is the impact wear velocity exponent of Wellinger model.

2.1.2 Rabinowicz (1995)

Rabinowicz studied the impact wear experimentally using a pendulum tester, with an impactor made from a hardened steel bearing, for testing different types of metallic materials (chromium, aluminum bronze, titanium, stainless steel AISI 304 and nickel) with different number of impacts (up to and including 2000 impacts). This led to the hypothesis that the wear during impact of ductile materials was similar to the wear of the same materials during sliding (adhesive) wear [17]. Attempting to achieve a quantitative measure of impact wear, Rabinowicz built a model (Equation 2) based on Archard's linear model [18], starting with the relationship:

$$W = \frac{kFx}{H_s} \tag{2}$$

where: W is the wear loss (mm³), F is the applied force (N), x is the sliding distance (mm), H_s is the hardness of the softer material (MPa), and k is a dimensionless sliding wear coefficient.

Equation 3 shows that the applied load can be represented by (F_r/μ), and $(F_r\ x)$ represents the energy dissipated during sliding. If ζ is defined as the total impact energy expended during slip and the term $(\zeta k/\mu)$ is replaced by a parameter K, then wear volume (W) is:

$$W = \frac{KeN}{H_s} \tag{3}$$

where K is the impact wear coefficient, e is the impact energy, and K is related to k by Equation 4:

$$K = \frac{k}{\mu} \tag{4}$$

2.1.3 Fricke & Allen (1993)

Fricke & Allen used a hammering-type impact wear apparatus to study the impact wear of different types of steel (AISI 304, 440C, 431, 817M40, 1210) under normal impact conditions with impact energies in the range 2-5J for 1000-100000 cycles. The authors proposed that impact wear results obtained from testing AISI 431 stainless steel specimens (line contacts, impact energy 2-5J, up to 50,000 impacts) can be represented by the impact wear model [19] represented by Equation 5, taking the same general form of those attempts to model erosion:

$$W = KNe^{n_{Fricke}} \tag{5}$$

where:

W is the wear volume loss (mm³), K and n_{Fricke} are the empirically determined impact wear coefficient and exponent respectively, and impact energy, e, and can be represented by Equation 6:

$$e = \frac{1}{2}MV^2 \tag{6}$$

Where M is the effective mass and V is the impact velocity (mm/s).

2.1.4 Lewis (2007)

Building on more applied work [3], Lewis developed a new, more general, predictive model [20] to measure the overall compound impact wear that comprises the sum of two wear models, one for sliding wear based on the work of Archard [18], and one for predicting impact wear, in the same form as used by Fricke [19], then modified by contact area ratio to the power j to account for changing contact geometry:

$$\mathrm{W} = \left(\frac{k\bar{F}Nx}{\mathrm{H}_s} + KNe^{n_{Lewis}}\right)\left(\frac{A_i}{A}\right)^j \tag{7}$$

where:

$\bar{F}$ is the average force (force/time) during impact (N),
k is the dimensionless sliding wear coefficient,
H_s is the hardness of the softer material (MPa),
N is the number of cycles,
K is the dimensional impact wear coefficient,
x is the sliding distance (mm),
n_{Lewis} is the impact wear exponent in Lewis model,
A_i is the initial elastic contact area as calculated by Hertzian analysis,
A is the contact area after N cycles,
j is the exponent of contact area ratio.

2.1.5 Akhondizadeh, Mahani & Rezaeizadeh (2013)

Akhondizadeh et al. used impact hammering wear rig to study the impact wear of steel plate impacted repeatedly by AISI 52100 steel balls and the mass loss is measured after 600 impacts. The impact velocity was varied between 2.5 - 10 m/s and with several ball radii used (7.5mm, 12.5mm, 20mm and 25mm). The results [21] suggest that the impact wear effectively depends on the impact velocity, impact angle, and ball size, thus a model was proposed based on those effective kinematic variables and is presented in the form:

$$\mathrm{W} = \mathrm{K}\, V^{\alpha}\, R^{\beta} e^{\theta\gamma} \tag{8}$$

where:

R is the ball radius (mm),
V is the impact Velocity (mm/s),
θ is the impact angle,
α, β, γ and K are the constant parameters.

This model was developed using Taguchi's Design of Experiment(s) (DoE) method but a limitation of this approach is that Taguchi assumes that there are no interactions between the factors, which is not necessarily the case for impact wear, especially for non-normal contacts.

Additionally, the number of cycles (impacts) is not taken into consideration which may reduce the accuracy of the model when compared to other approaches that include this to account for the total wear experienced in the contact.

2.2 Comparison of Models

It is important to note that material hardness has not been directly and explicitly considered as a parameter controlling the wear loss of materials under repetitive normal impact. It is often indirectly included, as part of experimentally derived coefficients and constants, from line fitting [20] or in the case of Rabinowicz [17] discounted because in that experimental work stainless steel experienced more wear than the aluminium alloys tested, despite stainless steel having higher hardness than aluminium.

Similar results were obtained by Fricke [19], who found that in a high carbon martensitic stainless steel (AISI 440C) with hardness of 710Hv there was more mass loss than in both austenitic stainless steel (AISI 304) (242Hv) and a high chromium martensitic stainless steel (AISI 431) (465Hv), leading to the same conclusion that hardness is not a primary parameter controlling the results of repetitive normal impact.

The models presented in Section 2.1 all share a significant limitation that they are unable to predict the wear loss by taking into account the effect of tangential force (shear force) during compound impact with different angles, especially at lower angles where more shear force than normal force is extant. Additionally, all those models depend on the total applied force, rather than both force components during compound impacts, so they are unable to predict as a function of impact angle.

The majority of previous models, with the exception of Lewis, do not consider the sliding component during impact and thus are more suitably applied to purely normal impacts. The Lewis model attempts to overcome this by means of its Archard-based sliding wear component, which is dependent on accurate knowledge of the magnitude of the interfacial sliding distance at the point of impact, but does not include the impact angle as an input directly. This is important because where impact wear occurs in many industrial applications, it is typically a compound impact (poppet valves, drilling tools, gears, bearings, linkages), yet as described here, no existing model can successfully predict the wear volume as a function of impact angle.

Using any of the previously developed impact wear models in these situations will clearly produce a ‘result’ but the accuracy of that will vary depending on the basis of the model and, for the majority, will be increasingly inaccurate the further from normal the impact is. This analysis of the state-of-the-art suggests, therefore, a real need to develop a simple, easily applied, model that can predict wear due to surface impingement at different impact angles. In particular, a model that can successfully predict impact wear loss with any impact angle to simulate the excessive wear that occurs at smaller impact angles, and thus leads to the under prediction of existing models, was the motivation for developing the new impact wear model that is described here.

2.3 Role of Impact Angle During Impact

In general, reducing the impact angle will lead to more tangential force (shear force), thus likely higher sliding that will potentially lead to more wear loss depending on the mechanical properties of the specimen. There appears to be no consensus in literature as to how this is defined, and in this work the impact angle (θ) is defined as the angle between the direction of impact caused by the impactor and the plane of the specimen, as illustrated in Figure 2.

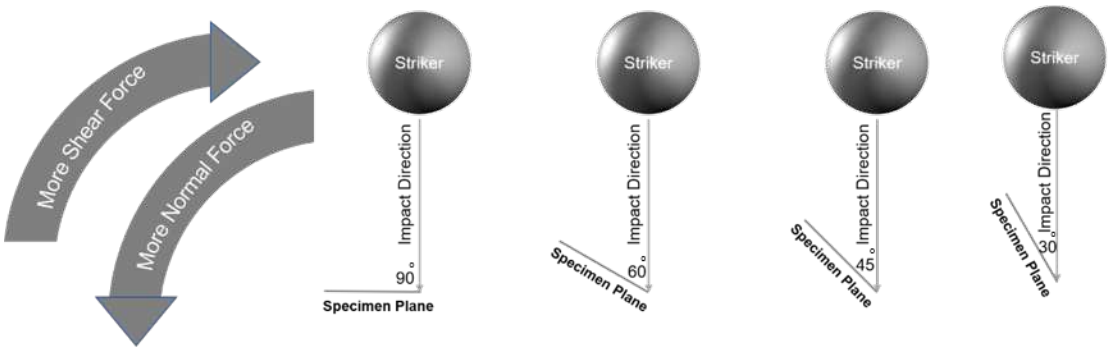

Figure 2 - Schematic diagram of different impact angles.

The impact angle also plays a key role in controlling the type of wear mechanism [22] in ductile materials. A larger impact angle will lead to more normal impact force than from a sliding impact, and damage is therefore more likely to be in the form of plastic deformation and surface fatigue due to spalling by surface cracking or delamination. However, a smaller impact angle will lead to more tangential force and less normal force, causing more abrasive wear in addition to spalling and subsurface cracks and leading to delamination and excessive material loss (wear). The experimental work of Akhondizadeh showed that the maximum wear loss occurred at 30°, where the shear and tangential components were at their highest [21].

Further investigation on the role of impact angle was conducted by Tyfour and colleagues [23] who saw impacts in the range 90°- 40° on a low carbon steel (A516-70) with a hardness of 145Hv. They used an in-house built impact hammering wear rig and the results indicated that the mass loss is highly dependent on the impact angle, with the lowest mass loss recorded with normal impact 0.1mg and highest mass loss at impact angle 40^0 0.7mg after 1000 cycles.

3 Proposed New Impact Wear Model

3.1 Statement of the Model

As discussed in Sections 2.2-2.3, a new model needs to consider the role of impact angle during impact. It is also considered that a model predicting compound impact can sensibly be divided into two components, as proposed by Lewis. Firstly, a component accounting for the normal impact, in a similar fashion to the models described in Section 2.1, but in terms of normal force rather than impact energy. Secondly, a component accounting for the non-normal (i.e. sliding) impact, in a similar fashion similar to the Archard equation, but in terms of tangential force rather than applied force. Both components then contribute to the total wear volume predicted for a compound impact. This approach also allows the model to be used to represent either normal or compound impact independently (by setting the component not of interest to zero) and also to be validated either separately or in combination.

Thus, the general form of the new model proposed here, described in more detail in Section 3.2.4, and subsequently referred to as the Zalzalah-Lewis-Slatter (ZLS) model, is as follows (Equation 9):

$$\mathrm{W} = \left(KNF_n{}^{n_{ZLS}} + \frac{kNxF_t{}^{m_{ZLS}}}{\mathrm{H}_s} \right) \tag{9}$$

where W is the wear loss (mm^3), K is the normal impact wear coefficient, N is the number of cycles, F_n is the normal component of impact force (N), k *is* the dimensionless sliding impact

wear coefficient, x is the sliding distance during compound impact (mm), F_t is the tangential (i.e. acting in the direction of the surface) component of impact force (N), H_s is the hardness of the softer material (nominally taken to be the specimen) (MPa), and n_{ZLS} and m_{ZLS} are the normal and sliding impact wear exponents.

The normal impact results of Fricke [19] show that AISI 440C (with a hardness of 710 HV) has more mass loss than AISI 304 (164 HV), 1210 (242 HV), and 817M40 (554 HV). Also, the results of zero wear paper for five different alloys [25] revealed that ductile cast iron (238 HV) has more mass loss than both AISI 304 (190 HV) and EN8 (213 HV). Therefore, hardness has not been considered as a primary parameter controlling the wear volume of different materials under normal impact, such approach is similar to the models described by Wellinger [12], (see Section 2.1.1) or Fricke [19], (see Section 2.1.3).

This model predicts wear volume and can be used with different impact angles (by use of the normal and tangential components of impact force) or solely for normal impact only (by using the normal component only (i.e. it is set to be the same as the impact force). It considers impact force, rather than impact energy, in order to be able to use measured impact forces for each impact, rather than impact energy calculated theoretically or derived from high-speed video camera data and to highlight the role of shear force during compound impacts. This may add benefit to the model as it can then account for any possible change the average peak impact force for a simulated contact due to change in the number of impact cycles.

The results presented by Wang et al. [24] revealed that the peak impact force slightly increased by a percentage of 7-9% during impact with significant increasing the number of cycles from 1000 to 100,000 cycles for different tested materials. However, it should be noted that the average peak normal impact force measured experimentally during this work (Section 3.2.1) did not change with different number of cycles and there was very small variation between tests.

3.2 Development of the Model

3.2.1 Experimental Method

The two components of the new model were derived from experimental work, initially austenitic stainless steel (AISI 304), with different angles of impact (normal (90°), 60° and 45°) and specific numbers of cycles (54,000) using an impact hammering wear rig developed, and used, in other work by Slatter [4-6], Bruce [9], and Zalzalah [25].

The rig is a cam driven, reciprocating-hammer type design, powered by a speed controlled (invertor) 1.1 kW electric motor. A striker holder at the end of the lever arm secures, in this case, a 15 mm diameter stainless AISI 52100 steel ball with a maximum surface roughness (Ra) 0.125μm which repeatedly impacts on the surface of the test specimen. The selection of this particular striker is arbitrary for the work conducted here, but it has been extensively used in the previous work performed on this apparatus where it was selected to be representative of the contact(s) being studied and shown to consistently reproduce measureable levels of wear needed for the development of the new model described here. The majority of the work presented in the literature, regardless of impacting method (hammer, projectile etc.), uses similar size and shape strikers because of the relative ease of achieving appropriate stresses, either side of yield, in the specimens made of common engineering metallic alloys in laboratory scale apparatus.

A summary of the mechanical properties for the AISI 304 used initially, the AISI 316 and EN8 used later, and the striker ball used throughout, is provided in Table 1.

Materials	**Yield Strength (σ_y) (MPa)**	**Tensile Strength (σ_u) (MPa)**	**Young's Modulus (GPa)**	**Measured Hardness (HV_{20})**
Austenitic Stainless steel (AISI 304)	270	581	190	190
Austenitic Stainless steel (AISI 316)	332	630	190	180
Medium carbon steel (EN8)	628	739	200	211
Ball (AISI 52100)	2000	2300	210	700-900

Table 1 - Summary of mechanical properties for the tested materials.

Although the three metal alloys used have relatively similar hardness, the EN8 has the hardness but least wear volume due to compound impact. Additionally, the tangential component of the new model has similar form of Archard equation [18] where the hardness of softer materials is inversely proportional to the wear volume.

The test specimens were 10mm thick discs cut from the same (for each material) 50mm diameter round bar. Each disc was then surface ground on both sides. There was no thermal treatment to relieve thermal stresses on specimens after the tests, in common with the literature. Before testing, the specimens were cleaned with compressed air, to remove any loose debris and dust, and isopropanol before being weighed using an electronic mass balance with accuracy to the nearest 0.1 mg.

All the specimens were impacted at a frequency of 10Hz and average impact velocity of 0.62m/s, as measured by high-speed camera (a Phantom V210), and impact energy of 0.23J, based on the effective mass of the overall hammer system of 1.19 kg. The maximum surface roughness (R_a) of the specimens was always less than 0.5 μm, as achieved by surface grinding. These test parameters were chosen because they result in easily measurable wear scars on the specimen surfaces and allow easy comparison with other work. Four repetitions were carried out for each test point. Specimens were tested randomly within a material group but no blinding was performed. The average peak impact force recorded experimentally using the load cell at a frequency of 10Hz under normal impact is 3476N with standard deviation of 8.8, based on that the other values of impact forces with 60° and 45° are shown in Table 2.

Impact Angle (θ)	Normal impact force F_n (N)	Tangential impact force F_t (N)
90°	3476	0
60°	3010	1738
45°	2457	2457

Table 2 - The value of both normal and tangential component of impact force with different impact angles at a frequency of 10Hz.

After each test, each specimen was cleaned with isopropanol to remove any possible remaining wear debris, dried, and then cleaned again with compressed air and reweighed using the same mass balance. Each specimen was weighed, used in a test, and reweighed on the same day. Then the mean wear volume was calculated based on the measured mass loss (i.e. the difference between the pre- and post- test mass measurements for each specimen) and

then converted to a volume using the mean measured material density, 7620 kg/m^3 and 7860 kg/m^3 for AISI 304 and 316 respectively and 7820 kg/m^3 for EN8.

The ball was selected to have a much higher hardness and strength than the specimens to ensure that the damage would mainly occur on the specimens (one-body wear), therefore, any damage to the striker ball has been neglected. That said, after each test the striker ball was changed for a new example.

3.2.2 Experimental Results

The experimental results revealed that increasing the tangential component leads to an increase in wear volume, as shown in Figure 3, and that the wear volume under normal impact is very small compared with that at 60° and 45°. The significant increase in wear volume that occurred with the non-normal angles used is considered due to the role of tangential component during impact. Despite the normal component decreasing with decreasing the impact angle, the wear volume increased significantly since the tangential components increased from 0 at normal impact to 2457N at impact angle 45°.

For the range of angles used in this work (90°- 45°), the highest wear volume always occurs at when the impact angle is 45°. This was found to be true for all of the test durations (number of cycles) studied. The impact angle strongly affects the wear volume loss of the material and often has more influence than the number of cycles (i.e. the total wear volume is more sensitive to impact angle than number of impact cycles). For example, in Figure 3, increases the number of cycles from 36,000 to 72,000 led to a 2.75x increase in wear volume by for normal impact 90°, 3x increase with compound impact 60°, and 3.2x with impact angle 45°. While changing the impact angle from normal 90° to 45° at any number of cycles such as 54,000 led to an 35x increase in wear volume.

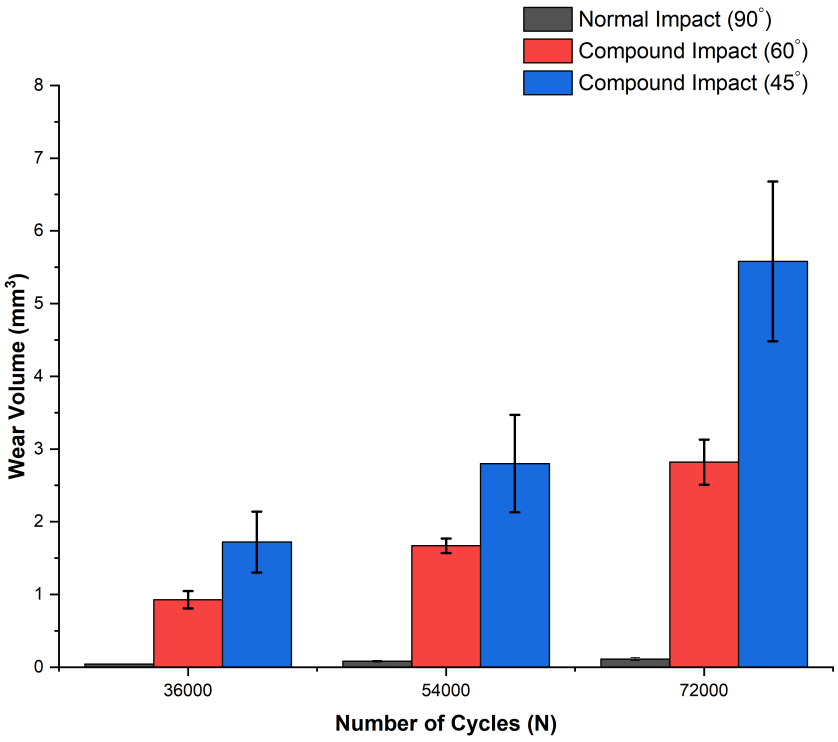

Figure 3 - Mean wear volume of AISI 304 as a function of impact conditions.

The sliding distance (x) that the striker slides against the inclined specimen surface of AISI 304 during impact was measured experimentally by using a high-speed camera. The sliding distance remained constant for each of the different numbers of impact cycles, for each angle. Due to the sliding distance being very small it was only realistic to obtain values due to the first impacts due to the decay of the reciprocating motion; therefore, six impacts were measured for each angle and the mean values were 0.35mm for 60° and 0.6mm for 45° with standard deviation of 0.05 and 0.03 respectively. This was compared with tests using an aluminium alloy, chosen due to its much smaller shear modulus and thus allow the striker to push through the material more easily, as the specimen material, and the mean sliding distances for a 60˚ and 45˚ impact were 0.44mm and 0.72mm respectively.

The three-dimensional morphology of typical impact wear scar is summarised in Figure 4 and illustrate the typical depth of the scar (up to 600 µm) as well as the plastic flow (up to 300 µm).

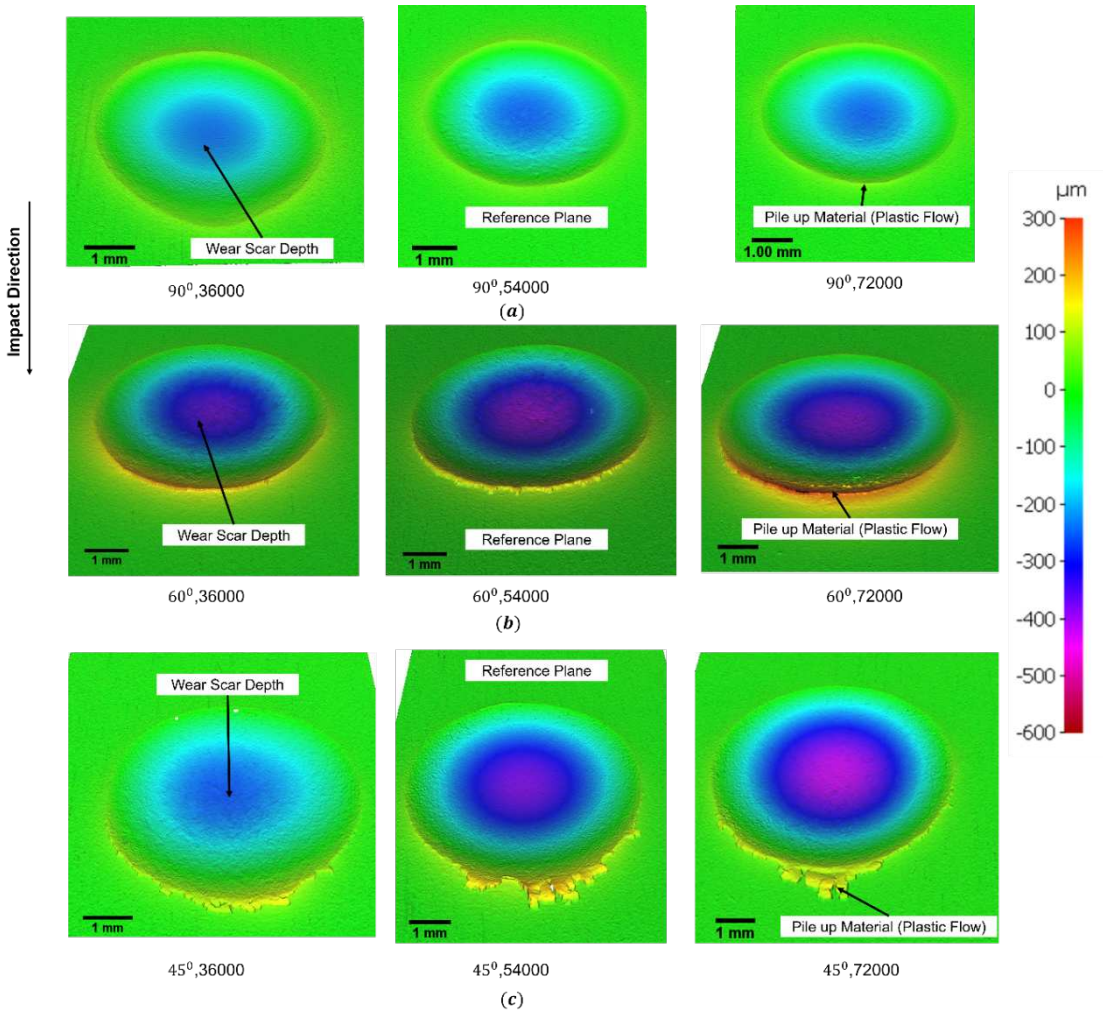

Figure 4 - 3D Image of typical depth and pile up profile of impact scars for material with different impact conditions: (a) under normal impact 90°, (b) with impact angle 60°, (c) with impact angle 45°.

Differences could be observed in all the scars among the range of applied parameters, with an increase in the number of cycles leading to a slight increase in the amount of plastic flow on the impact wear scars and a small increase in the impact wear scar size.

The green regions in Figure 4 indicate the reference plane of the scanned surface, while the positive surface above the reference plane (yellow and orange regions) represents the pile up

materials and the negative surface below the reference plane (turquoise, blue and purple regions) represents the depth of impact wear scar.

Figure 4 shows that increasing the number of cycles led to a slight increase in both depth and pile up of scar materials under normal impact, while changing the impact condition from normal to compound impact caused a significant amount of plastic flow to form at the bottom edge. This was due to plastic deformation and impact direction and accompanied by a noticeable increase in wear scar depth. It also shows that the pile up materials (plastic flow) are uniform in shape at the bottom edge with an impact angle of 60°, while with an impact angle of 45° it was extruded outside the contact region. by the effect of higher shear forces. Two different techniques were used (spherical and rectangular plane) and both methods consistently produced the same results.

Further investigation using specimens manufactured from a medium carbon steel (EN8) and another common type of austenitic stainless steel (AISI 316) and the same methodology and number of cycles (54,000) in order to use material type as the primary independent variable, also revealed a similar trend to that exhibited by AISI 304, with more wear volume loss occurring at 60° and the largest volume at 45° as shown in Figure 5.

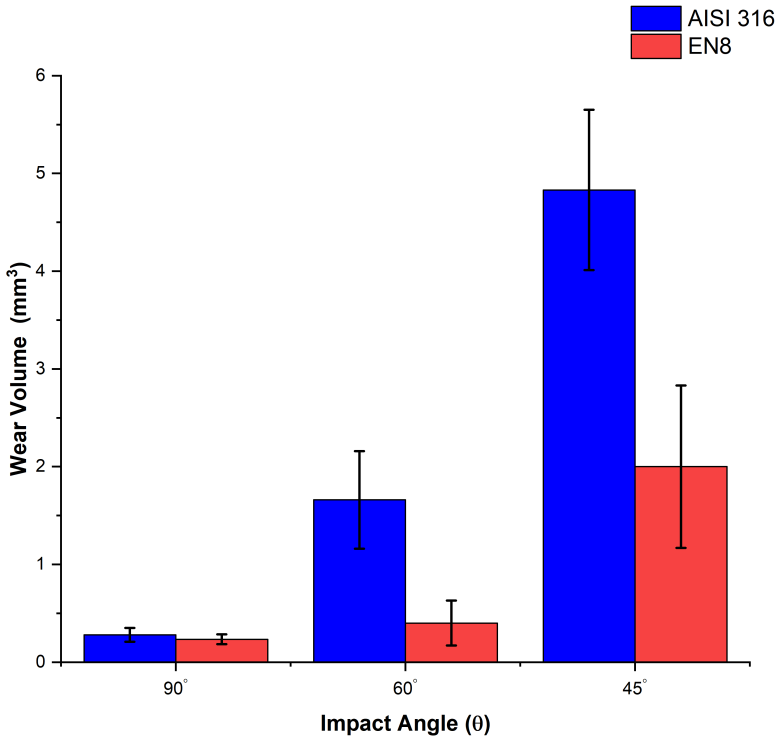

Figure 5 - Mean wear volume of AISI 316 and EN8 as a function of impact angle with specific number of cycles (54000).

Figure 5 indicates that changing the impact angle from normal (90°) to compound (60° and 45°) led to an increase in material loss and that the wear conditions became more aggressive. The sliding component plays an important role in material loss as the highest material loss occurred at an impact angle of 45°, similar to the results for AISI 304 presented in Figure 3.

The standard deviation of the results shown in Figure 3 and Figure 5 is in similar range to that previously reported by Slatter [4-6].

3.2.3 Discussion of Results

Based on data from experiments with the two austenitic stainless steels and the medium carbon steel, there is a correlation between wear volume and number of cycles (Figure 3) and increasing sliding distance during compound impact leads to an increase in wear volume. This is inversely proportional with hardness of impacted materials, since medium carbon steel has the highest hardness among the tested materials and showed lower wear volume compared with both types of austenitic stainless steel in agreement with the Archard equation [3].

The repetitive normal impact of AISI 304 revealed that increasing the impact force will always lead to an increase in wear volume. Similar results were found with both AISI 316 and EN8, leading to a correlation between impact force and wear volume for different materials (Figure 6).

Under compound impact, the premise of two components appears valid, however it is important to note that for a compound impact against AISI 304 the majority (96%) of wear volume contributed to by the tangential component and the normal component the remainder. This result is likely due to that under normal impact the wear loss was very small compared with compound impact because of the zero wear volume. Previously defined [25] by the authors of this present work, zero wear volume is the volume previously occupied by material that appears to have been deformed by impact, causing its surface to be at a different point in space, but remains in the contact zone (i.e. the wear volume change due to material compression before any mass loss occurs). This appears to account for the majority of volume loss for AISI 304 under normal impact.

3.2.4 Derivation of Model Parameters

Normal Impact Component

Wear coefficients K and exponent n_{ZLS}, which represent the normal impact conditions are shown in Table 3.

Material	K	n_{ZLS}
AISI 304	1.85×10^{-9}	0.816
AISI 316	5.64×10^{-9}	0.816
EN8	2.04×10^{-8}	0.655

Table 3 - Normal impact wear coefficient and exponent n for tested materials

These were calculated from the experimentally derived relationship between the measured impact force (1982 N, 2783 N, and 3476 N) and wear volume by specific number of cycles (54,000), using a line fitting method similar to the work of Wellinger [12] and Fricke [19]. Figure 6 shows this derivation of the normal component of tested alloys with an impact angle of 90° and the error bars represents the standard deviation from four repetitions of the data.

This number of cycles was selected to obtain measurable wear volume with all impact forces whilst minimizing test length. That said, however, the wear volume due to normal impact is still a very small proportion of the total wear (Figure 3) due to the role of zero wear volume in this type of contact (as described elsewhere [25]).

The normal component of the new model is in terms of normal impact force which differs the approaches of Willinger [12] (velocity based) or Fricke model [19] (energy based) Fricke used impact energy, rather than impact velocity, in order to include the effective mass in the model. From that perspective, and since the impact force is the resultant of effective mass

multiply by the acceleration of impact, the normal component of the new model is different from the previously developed models since it considers the acceleration of impact rather than impact velocity or energy.

Sliding due to Impact Component

Due to the paucity of data in the literature describing wear as a function of tangential force for the tested alloys, experiments to derive the sliding impact wear coefficient k and exponent m_{ZLS} to be used in the new model, were conducted only using AISI 304 specimens, as data from experiments using other materials would not be able to be then validated against the work of others (as it does not exist). That said, in order to give confidence in the data from these experiments conducted for this work the results were compared with the experimental work of Rigaud [25] using the same material and also at impact angles of 60°, 45° and 30°.

The tangential component was derived using similar line-fitting approach as for the normal component with both impact angles used (60° and 45°) gives values for k of 1.45 $\times 10^{-7}$ and for m_{ZLS} of 1.85. It should be noted that because a uniaxial load cell was used throughout this work, the tangential forces (1738N for 60° impacts and 2457N for 45° impacts) were calculated theoretical from the normal forces recorded experimentally.

Confidence in the model would be increased by using more angles to those used here (60° and 45°) to provide more data points for the tangential component of the model. In the case of the apparatus used here changes to the configuration of the striker and striker holder are required to provided alternative fixed configurations or a variable system that can facilitate different angles at which impacts can occur. Similarly, using other materials would improve the efficacy of the model by generating different impact wear coefficients and exponents. That said, however, with only two compound impact angles the model shows good agreement under compound impacts with other number of cycles (36,000; 72,000) to the one the model was derived (54,000) (Section 5.3 and Figure 12 (a)).

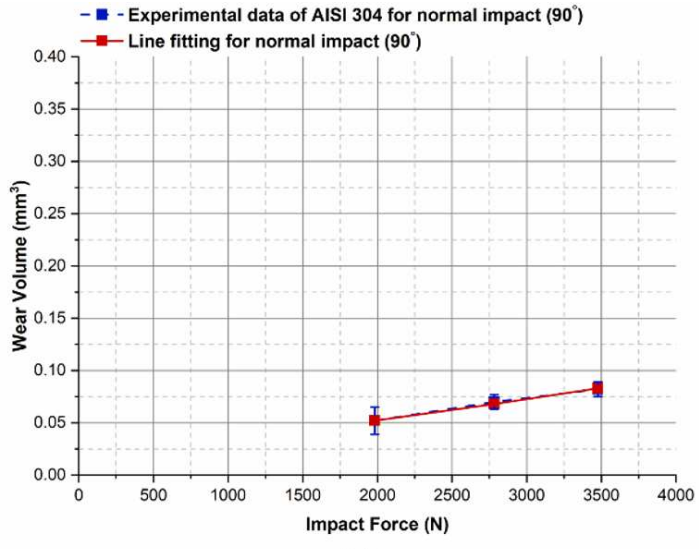

(a)

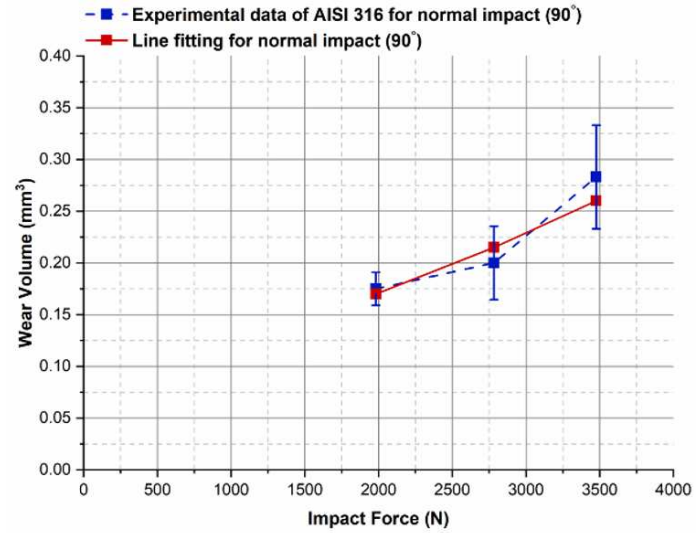

(b)

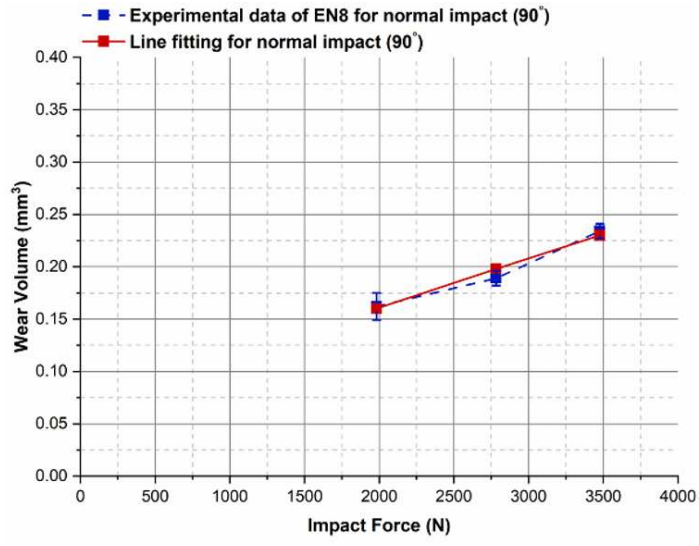

(c)

Figure 6 – Line fitting from the experimental data of (a) AISI 304, (b) AISI 316 and (c) EN8 under normal impact after 54,000 cycles.

4 Validation of the Model

4.1 Austenitic Stainless Steel (AISI 304)

The new model proposed here was validated with experimental results from literature [26] under different impact angles using the same exponents n_{ZLS} (0.816), m_{ZLS} *(1.85)* and wear coefficients K (1.85×10^{-9}) and k (1.45×10^{-7}), since the same material was being used. A comparison is provided in Figure 7 and shows some deviation between the experimental data and the new model with different impact angles and specific number of cycles (560,000).

The deviation between the experimental data of Rigaud and this new model is likely to be as a result of large differences between the number of cycles reported in literature and the actual number of cycles accumulated (e.g. a mismatch between nominal excitation frequency and actual impact frequency). This indicates that the dynamical system is strongly nonlinear and the rig is unstable during tests caused by vibration during impact and induced dispersion in impact location, as described by Rigaud, which may reduce the wear volume significantly since the impact is not occurring in exactly the same contact region.

It is also possible that variation in surface roughness could influence sliding impacts, even if that effect in a very small scale. Liang [27], for example, found that the wear volume of materials increased from 1 mm^3 with a surface roughness of R_a=0.1µm to 3 mm^3 with surface roughness R_a=0.5 (within the range of the work presented here).

Lastly, the experimental data of Rigaud has not been repeated which reduce the accuracy of the results. This deviation between the experimental data and the model data should be considered against very small predicted values for both approaches (less than 0.008 mm^3).

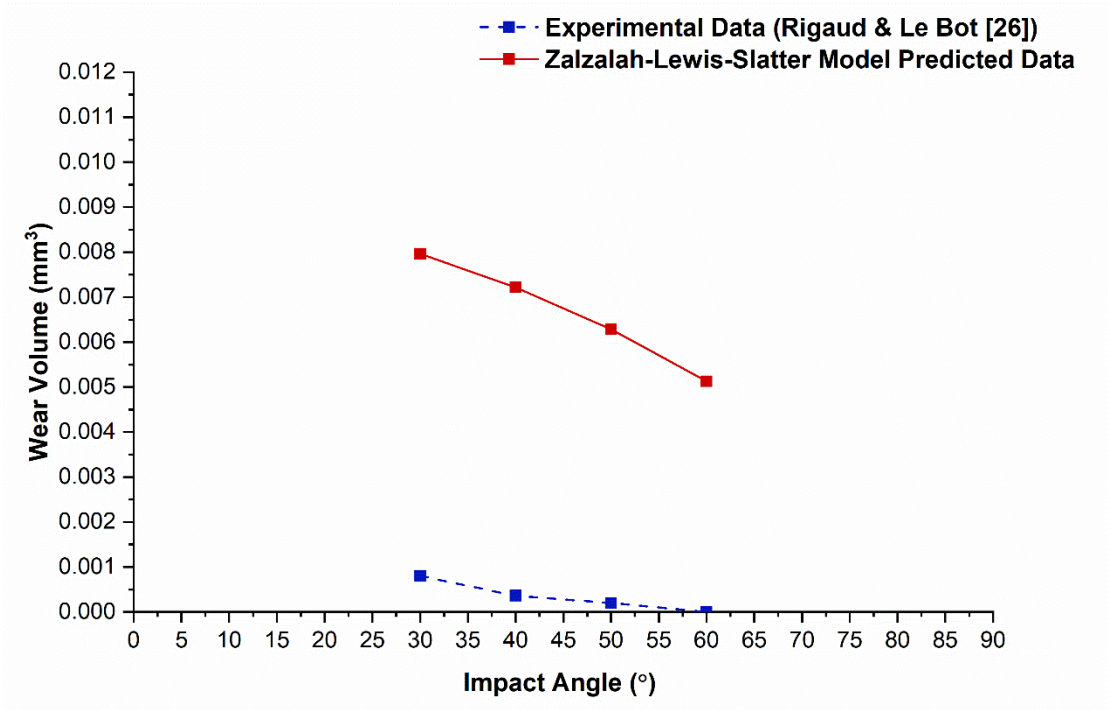

Figure 7 - Experimental data of Rigaud & Le Bot [26] compared with the Zalzalah-Lewis-Slatter model data.

4.2 Austenitic Stainless Steel (AISI 316)

Validations using data from published experiments using AISI 316 were limited to using the normal component of the new model because of a lack of information about the tangential impact force in those studies. Experimental data from testing of unburnished specimens (310 Hv) and burnished specimens (405 Hv) from a study by Yilmaz & Sadeler [28] was compared with the new model (Figure 8). In that work, the specimens are being subjected to normal impact (impact force 560 N for 1000, 10,000, and 100,000 impacts).

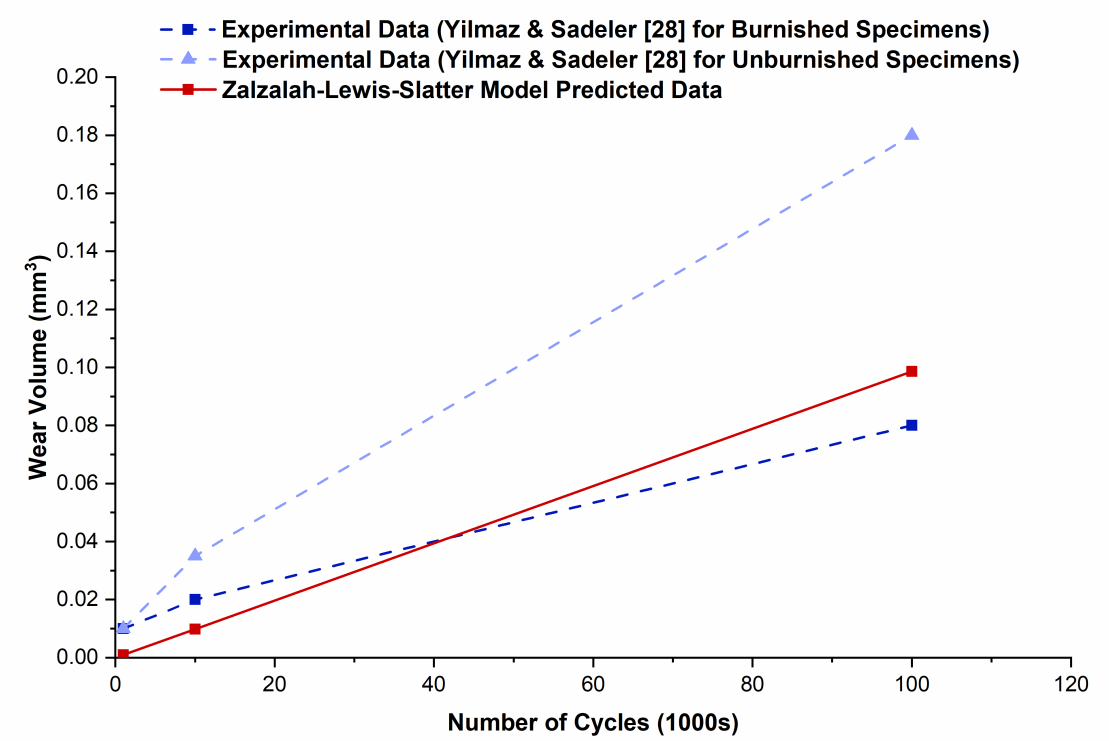

Figure 8 - Experimental data of Yilmaz & Sadeler [28] under normal impact compared with Zalzalah-Lewis-Slatter model data.

Very good correlation was found with the data reported for the burnished specimens but much weaker for the unburnished. This can be attributed to the fact that the new model, in common with the other extant models described in Section 2, is based on wear volumes derived from measured mass loss (Figure 3) rather than the 3D non-contact profilometry used by Yilmaz & Sadeler. As described in Section 3.2.3 means that the latter method will detect the extra volume loss resulting from zero wear. Having been subjected to mechanical working, the burnished specimens will likely not experience significant zero wear phenomenon, thus the wear reported by 3D non-contact profilometry will be the same as that detected by the measured mass loss method. The model output was compared with the data of burnished and unburnished specimens despite their differences in bulk hardness because hardness in not an input parameter for the model in normal impact conditions (Equation 9).

4.3 Medium Carbon Steel (EN8)

Two validations were possible with medium carbon steel as the material of interest, and with normal impact conditions using the normal impact wear coefficient K and impact force exponent n_{ZLS} (2.04×10^{-8} and 0.655, respectively) derived experimentally in this work (Section 3.2.4). Figure 7 shows good correlation between the predictions of the new model and the experimental data from the work of Jiang et al. [29] where rail steel and a welded rail steel joint (Figure 9) were subjected to normal impact.

The experimental results here were based on impact force of 200N and different number of impact cycles (5,000-100,000) compare favourably the predictions of the new model, particularly for data points representing wear occurring after large numbers of cycles. The disparity between the experimental data and the predictions at lower numbers of cycles is again due to the role of zero wear, in this case because of the use of the spherical cap method which leads to results similar to the 3D non-contact profilometer, albeit with greater potential error. That said however, the better correlation of the model to towards the 'end of life' is more preferable in an industrial context where total wear life is often of more immediate interest than the evolution of the early stages of wear, especially in contacts where that stage is effectively used as a running in period.

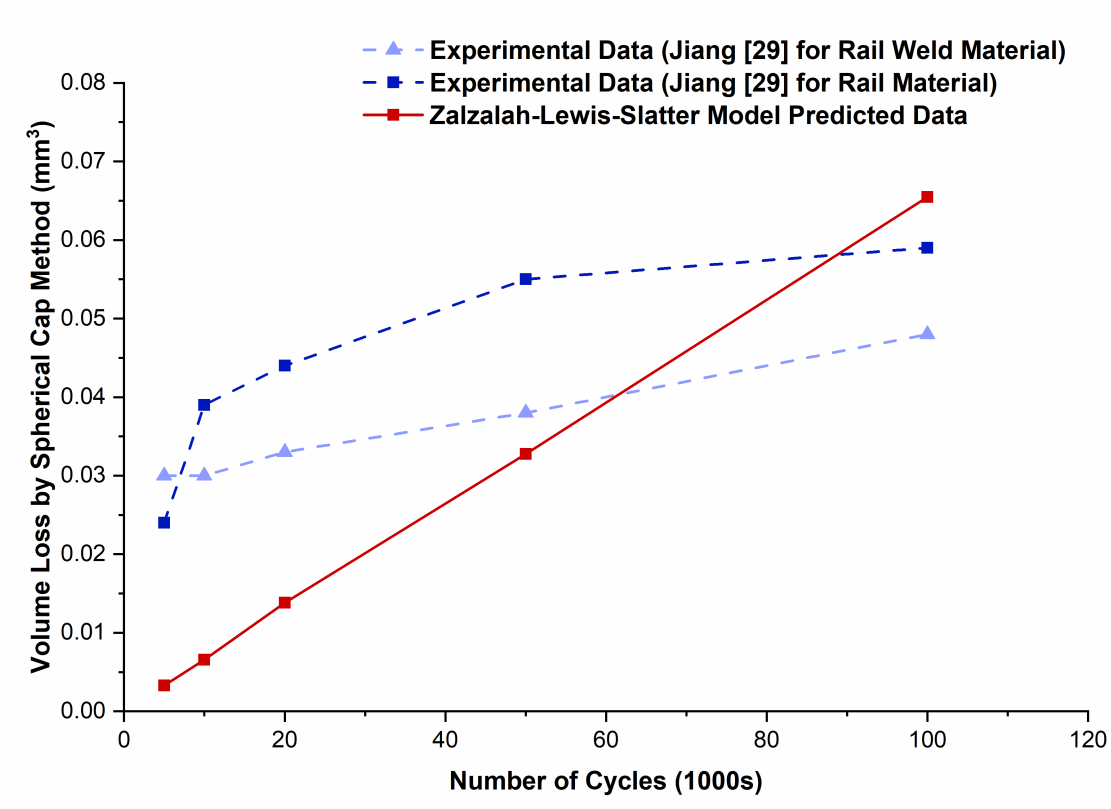

Figure 9 - Comparison between the experimental data of Jiang et al. [29] for steel of rail material and rail weld joint material and data from Zalzalah-Lewis-Slatter model data.

A second validation was carried out between the new model's predictions and the experimental data of volume loss obtained by Wang et al. [30] for 40Cr steel impacted normally (impact force of 80.9N, and up to 100,000 cycles). This is shown in Figure 10 and is similar to the comparison made with the unburnished AISI 316 results (Figure 8) in that the

new model under-predicts due to the difference between measurement methods, in this case 3D non-contact profilometer, and thus neglecting zero wear volume.

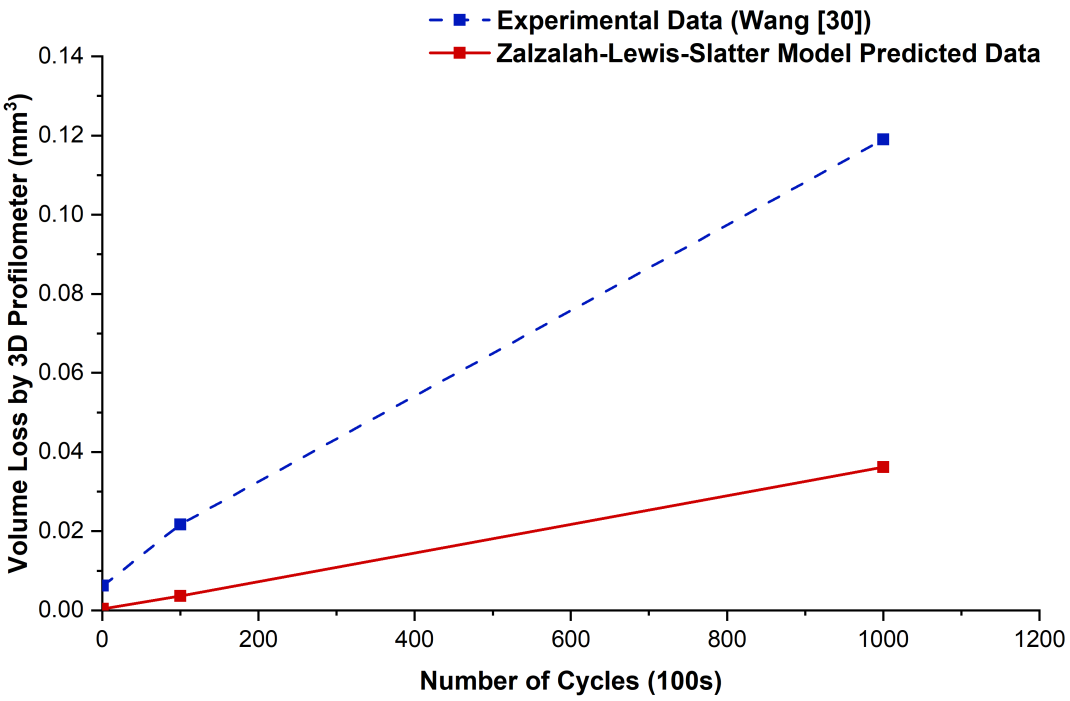

Figure 10- Experimental data of 40Cr steel from Wang [30] [4] compared with the Zalzalah-Lewis-Slatter model data.

5 Efficacy of the Proposed New Model

5.1 Complexity and Ease of Use

The new Zalzalah-Lewis-Slatter model proposed here was developed based on specific parameters (number of cycles, normal and tangential impact force, sliding distance and hardness of softer material) to reflect information readily known about contacts in many real mechanical systems. This means that it can be easily used for predicting both normal and compound impact wear, including angle as a function, without requiring large number of experimentally derived parameters that often need apparatus not always found outside dedicated research facilities.

5.2 Range of Materials

The model can be used under both normal and compound impact and the results easily compared with other data to obtain accurate values for the wear volume. Existing experimental data representing the behaviour of three widely used metal alloys has been successfully used to validate its predictions for normal and compound impact. It is important to note that none of the experimental work from literature used for validation described any data robustness information (as previously discussed [31]) could have affected the accuracy of the wear volume results, but nonetheless good correlation was generally found with the model. Further experimental to fully validate the experimental data and subsequent model parameters for materials other than AISI 304 is also required.

5.3 Impact Conditions and Mechanistic Phenomenon

All the results were obtained with dry contacts since most impact wear applications fall within this field, hence the role of lubricant has not been taken into consideration during this work. Further work is required to understand the role of a lubricant, or other third body in transmitting the force applied in the impact. The model could also be developed to include the role of work hardening directly and then compared with other experimental data. However, additional experimental parameters will be required, such as work hardening exponents for each material perhaps collated together as a library, as such trends are not easy to compare and validate.

The model is expected to lead to better correlation with the wear volume results obtained by the de facto standard of mass loss (converted to wear volume by considering the material's measured density) than with data obtained via direct volume measurement methods especially under normal impact.

Table 4 shows the differences in volume losses data produced under normal impact (90°) on the AISI 304 specimens and measured by mass loss (wear volume) and 3D non-contact profilometer (total volume loss) with different number of cycles at impact force of 3476N. While Figure 9 shows the differences in results between the model and these experimental data which is mainly contributed to the role of zero wear volume during normal impacts [25].

Conditions	Mean Wear Volume V_w (mm^3)	Standard Deviation σ (STD)	Mean Total Volume Loss V_t (mm^3)	Standard Deviation σ (STD)
36000, 90°	0.042	0.0066	2.08	0.16
54000, 90°	0.082	0.012	2.1	0.18
72000, 90°	0.111	0.02	2.18	0.2

Table 4 - Mean wear volume and total volume loss of AISI 304 under normal impact with different number of cycles

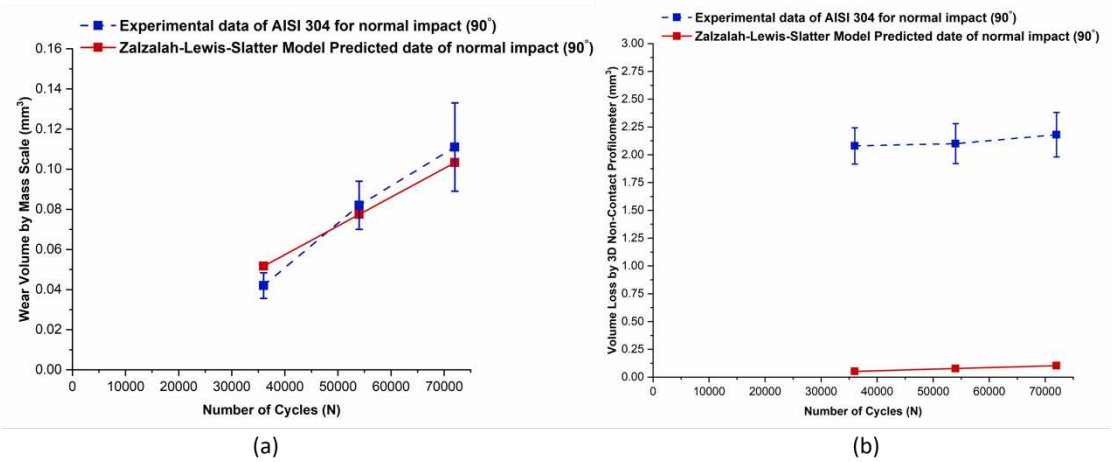

Figure 11 – Comparison between the model and the results obtained during this study for AISI 304 under normal impact and impact force 3476 N where; (a) wear volume measured by mass scale and (b) volume loss measured by 3D non-contact profilometer

Figure 11 (b) shows large deviation between the experimental data of AISI 304 measured directly by 3D non-contact profilometer and the model (based on wear volume). While this deviation is contributed to the role of zero wear volume, it reduced significantly with compound impact (60° and 45°) as shown for example in Figure 12 with an impact angle of 60°.

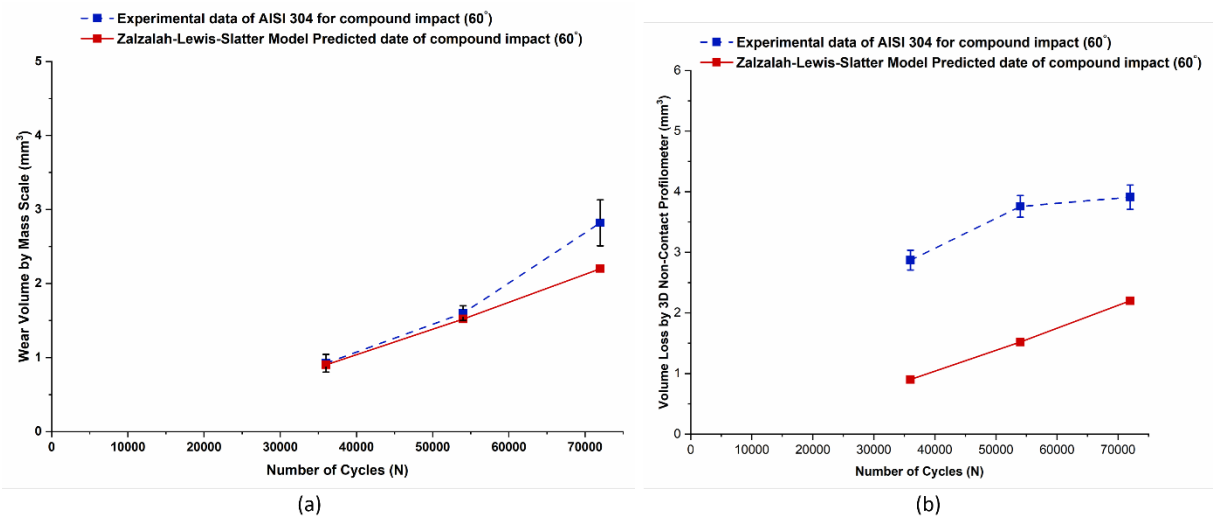

Figure 12- Comparison between the model and the experimental results of AISI 304 under compound impacts and impact force of 3476N where; (a) wear volume measured by mass scale and (b) volume loss measured by 3D non-contact profilometer.

The majority of deviation seen in Figure 12 (b), is contributed to the plastic flow volume that removed from the centre of wear scar and accumulated near the bottom edge (Figure 4 (b)) and minimising the effect of zero wear volume during compound impact. Figure 11 (a) and Figure 12 (a) show an excellent correlation between the experimental data of AISI 304 and the model under both normal and compound impacts with different number of cycles (36,000 and 72,000) to that the model was initially derived (54,000). This comparison and deviation is similar to that achieved by Fricke (between the experimental data of AISI 431 and the model with different number of cycles [2]) and provides further validation of the model for both normal and compound impacts.

The new model is based on wear volume measured by mass loss, rather than total volume loss measured by 3D non-contact profilometer. This is the typical method for measuring the wear volume, calculating the impact wear coefficient, and comparing it with other values from extant wear models. Also, this method is similar to all the extant wear models described in Section 2.1 (that are based on mass loss). A 3D non-contact profilometer directly measures the total volume loss, not the wear volume, thus does not necessarily reflect the wear resistance performance of materials under investigation.

The model does directly consider the role of friction during impact in that the contact between the ball and the specimen is considered as a frictionless during normal impact as with Hertzian theory [32]. This is commonplace in literature where most authors neglect the friction during normal impacts and set it to zero, for example in the work of Rigaud [26].

Considering the tangential component of the model, studies show that there is no simple model that can be used to determine the actual coefficient of friction during contact [33] due to friction being a system property. Studies also show that the coefficient of friction for AISI 304 can be changed by using different applied load, sliding speed or number of cycles and thus will lead to different values of the coefficient of friction [33-35].
A further study by Rigaud [26] revealed that change the impact angle will eventually lead to different value of coefficient of friction. This suggests that is non-trivial to include the role of friction in the model.

Lastly, the results showed that the impact wear coefficient K and sliding wear coefficient k of the tested materials both achieved values to an exponent in the range 10^{-7}-10^{-9}, potentially indicating the severity of wear during impact, where a value of 10^{-2} indicates very severe wear conditions and a value of 10^{-9} indicates that the wear conditions are far less aggressive [36-38]. This means that these materials could be considered as materials with good impact wear resistance within the impact conditions explored, and a value of 10^{-5} and 10^{-6} could indicate moderate wear conditions [17, 19, 39].

6 Conclusions

The following conclusions can be drawn from this work;

- A new model for predicting both normal and compound impact wear taking into consideration the role of shear force (tangential force).
- The model has with good agreement using data obtained from literature describing studies that considered normal and compound impacts on similar engineering alloys.
- The model correlates better wear volume data measured indirectly by mass scale (the de facto standard) than direct methods due to the role of zero wear.

It should also be noted that this new model could be improved further to include directly the role of work hardening (rather than it being 'hidden' in experimentally derived wear coefficients) and zero wear. This would lead to better correlation with a wider range of experimental data presented in the literature, however but this may not be easy to achieve with the typical information provided therein. Similarly, the model has been validated under compound impact for only one material (AISI 304) due to lack of data from other materials in the literature and further experimental work for materials other than AISI 304 is required to fully validate the model and its parameters

Acknowledgements

Mohanad Zalzalah would like to acknowledge the support of: Iraqi Ministry of Oil and LUKOIL.

References

1. P. Engel, "Percussive impact wear: A study of repetitively impacting solid components in engineering," Tribology International, vol. 11, pp. 169-176, 1978.
2. R. Lewis, C. Tsoraki, J. Broughton, J. Cripps, S. Afodun, T. Slatter, et al., "Abrasive and impact wear of stone used to manufacture axes in Neolithic Greece," Wear, vol. 271, pp. 2549-2560, 2011.
3. R. Lewis, R. Dwyer-Joyce, "Wear of diesel engine inlet valves and seat inserts," Proceedings of The Institution of Mechanical Engineers (Part D: J Automobile Engineering), vol 216, 2002.
4. T. Slatter, H. Taylor, R. Lewis, and P. King, "The influence of laser hardening on wear in the valve and valve seat contact," Wear, vol. 267, pp. 797-806, 2009.
5. T. Slatter, A. H. Jones, R. Lewis, “The influence of induction hardening on the impact wear resistance of compacted graphite iron (CGI)”, Wear, vol. 270 (3-4), pp. 302-311, 2011.
6. T. Slatter, A. H. Jones, R. Lewis, “The influence of cryogenic processing on wear on the impact wear resistance of low carbon steel and lamellar graphite cast iron”, Wear, vol. 271 (9-10), pp. 1481-1489, 2011.
7. F. Lai, S. Qu, Y. Duan, R. Lewis, T. Slatter, L. Yin, et al., "The wear and fatigue behaviours of hollow head & sodium filled engine valve," Tribology International, vol. 128, pp. 75-88, 2018.
8. R. H. Staunton, D. F. Cox, "Ageing and Service Wear of Spring-Load Pressure Relief Valves Used in Safety-Related Systems at Nuclear Power Plants", U.S. Nuclear Regulatory Commission, 1995.
9. T. Bruce, H. Long, T. Slatter, and R. Dwyer-Joyce, "Formation of white etching cracks at manganese sulfide (MnS) inclusions in bearing steel due to hammering impact loading", Wind Energy, vol. 19, pp. 1903-1915, 2016.
10. K. J. Swick, G.W. Stachowiak, A.W. Batchelor, "Mechanism of wear of rotary-percussive drilling bits and the effect of rock type on wear", Tribology International, vol. 25, pp. 83-88, 1992.
11. S. Ge, Q. Wang, J. Wang, "The impact wear-resistance enhancement mechanism of medium manganese steel and its applications in mining machines", Wear, 376-377, pp. 1097-1104, 2017.
12. K. Wellinger and H. Breckel, "Kenngrössen und verschleiss beim stoss metallischer werkstoffe," Wear, vol. 13, pp. 257-281, 1969.
13. Hutchings, R. Winter, and J. E. Field, "Solid particle erosion of metals: the removal of surface material by spherical projectiles," Proceedings of the Royal Society of London. A. Mathematical and Physical Sciences, vol. 348, pp. 379-392, 1976.
14. Finnie, "Some observations on the erosion of ductile metals," Wear, vol. 19, pp. 81-90, 1972.

15. R. Lewis, M. Zalzalah, and T. Slatter, "Impact Wear Failures," in “ASM Handbook Vol. 11 - Failure Analyhsis & Prevention” Editors; B. Miller et al., ASM International, pp730-744, 2021.
16. K. Guo, C. Tian, Y, Wang, Y. Wang, W. Tan, "An energy-based model for impact-sliding fretting wear between tubes and anti-vibration bars in steam generators", Tribology International, vol. 148, 2020.
17. E. Rabinowicz, "Friction and Wear of Materials," 1995.
18. J. Archard, "Contact and rubbing of flat surfaces', Journal of Applied Physics," 1953.
19. R. Fricke and C. Allen, "Repetitive impact wear of steels," Wear, vol. 162, pp. 837-847, 1993.
20. R. Lewis, "A modelling technique for predicting compound impact wear," Wear, vol. 262, pp. 1516-1521, 2007.
21. M. Akhondizadeh, M. F. Mahani, M. Rezaeizadeh, and S. Mansouri, "Propose a New Model for Prediction of the Impact Wear Using an Experimental Method," Journal of Solid Mechanics Vol, vol. 5, pp. 245-252, 2013.
22. G. Stachowiak & A. Batchelor, “Engineering Tribology (3rd Edition)”, Butterworth-Heinemann, 2005.
23. W. I. R. Tyfour, M. T. Hayajneh, and R. Hendawi, "Role of impact angle reversal on impact wear of mild steel," Proceedings of the Institution of Mechanical Engineers, Part J: Journal of Engineering Tribology, vol. 232, pp. 97-105, 2018.
24. Z. Wang, Z.-b. Cai, Z.-q. Chen, Y. Sun, and M.-h. Zhu, "Low-velocity impact wear behavior of ball-to-flat contact under constant kinetic energy," Journal of Materials Engineering and Performance, vol. 26, pp. 5669-5679, 2017.
25. M. Zalzalah, R. Lewis, T. Slatter, “Defining the role of ‘zero wear volume’ in percussive impact”, Wear, vol 464-465, 2021.
26. E. Rigaud and A. Le Bot, "Influence of incidence angle on wear induced by sliding impacts," Wear, vol. 307, pp. 68-74, 2013.
27. G. Liang, S. Schmauder, M. Lyu, Y. Schneider, C. Zhang, and Y. Han, "An investigation of the influence of initial roughness on the friction and wear behavior of ground surfaces," Materials, vol. 11, p. 237, 2018.
28. H. Yilmaz and R. Sadeler, "Impact wear behavior of ball burnished 316L stainless steel," Surface and Coatings Technology, vol. 363, pp. 369-378, 2019.
29. W. Jiang, C. Liu, C. He, J. Guo, W. Wang, and Q. Liu, "Investigation on impact wear and damage mechanism of railway rail weld joint and rail materials," Wear, vol. 376, pp. 1938-1946, 2017.
30. J. Wang, L. Lu, and Z. Ji, "A Study on the Impact Wear Behaviors of 40Cr Steel," Tribology Online, vol. 10, pp. 273-281, 2015.
31. M. Watson, et al., “An analysis of the quality of experimental design and reliability of results in tribology research”. Wear, 426-427, 1712-1718, 2019.
32. K. L. Johnson, Contact Mechanics: Cambridge university press, 1987.

33. G. Chen, "3-Fundamentals of Contact Mechanics and Friction," Handbook of Friction-Vibration Interactions, pp. 71-152, 2014.
34. Z. Yang, M. Naylor, and D. Rigney, "Sliding wear of 304 and 310 stainless steels," Wear, vol. 105, pp. 73-86, 1985.
35. M. CHOWDHURY, D. NURUZZAMAN, and R. Biplov, "Experimental investigation of friction coefficient and wear rate of stainless steel 304 sliding against smooth and rough mild steel counterfaces," Gazi University Journal of Science, vol. 26, pp. 597-609, 2013.
36. J. A. Williams, "Wear and wear particles—some fundamentals," Tribology International, vol. 38, pp. 863-870, 2005.
37. J. Challen, P. Oxley, and B. Hockenhull, "Prediction of Archard's wear coefficient for metallic sliding friction assuming a low cycle fatigue wear mechanism," Wear, vol. 111, pp. 275-288, 1986.
38. E. Rabinowicz, "The wear coefficient—magnitude, scatter, uses," 1981.
39. L. Yang, "A test methodology for the determination of wear coefficient," Wear, vol. 259, pp. 1453-1461, 2005.